Supporting Information

Naturally nano: Synthesis of versatile bio-inpired monodisperse microspheres from *Bacillus* spores and their applications

Zhiming Zeng[a], Yin Zhong[a], Huicui Yang[a], Ruihua Fei[a], Rui Zhou[a], Rafael Luque[b], Yonggang Hu[a]**

[a]*State Key Laboratory of Agricultural Microbiology and College of Life Science and Technology, Huazhong Agricultural University, Wuhan 430070, China, E-mail: Yongganghu@mail.hzau.edu.cn*

[b]*Departamento de Quimica Organica, Universidad de Cordoba, Campus de Rabanales, Edificio Marie Curie (C-3), Ctra Nnal IV-A, Km 396, E14014, Cordoba (Spain), E-mail: q62alsor@uco.es*

Keywords: monodisperse microparticle, *Bacillus,* spore, nature-inspired, noble metal nanoparticle

Properties of TSs

Furthermore, the morphology of parent TSs was also preserved after storage in H_2O_2 (≤ 20%) solution after one day as well as after O_2 treatment at high-pressure (0.1–0.3 MPa) after 2 h. This stability may be beneficial to the use of spore-based microspheres in aqueous reaction systems with high-pressure and highly oxidizing environments.

Adsorption experiments

The power-time curves for the adsorption of Au NPs by TSs were corrected by subtracting the dilution heat (Figure 2G). The adsorption enthalpy change (H_{ads}) was calculated by the following equation: $Q_{ads}= V_s\, q^*\Delta H_{ads}$ (1)

Where Q_{ads} (kJ) is the net heat for the interactions of Au NPs with TSs, V_s (L) is the volume of TSs suspension, and q^* (M) is the amount of Au NPs. As shown in Figure 2G1, ΔH_{ads} values ranged from –884 kJ mol^{-1} Au to –78 kJ mol^{-1} Au. A relatively strong covalent interaction between Au NPs and TSs was also confirmed by ITC due to the product of large ΔH_{ads} values.

The equilibrium adsorption of Au NPs on TSs was determined. As shown in Figure 2H, there was a gradual increase of adsorption for Au NPs until the equilibrium was attained. An equilibrium concentration of Au NPs was reached at about 18 mg L^{-1} for TSs. The adsorption isotherms of Au NPs on TSs conformed to the BET equation:

$$v = \frac{v_m c x}{(1-x)} \times \frac{1-(n+1)x^n + n x^{n+1}}{1+(c-1)x - c x^{n+1}} \quad (2)$$

Where v is the amount of Au NPs adsorbed per unit weight of TSs at equilibrium concentration (mg g^{-1}), v_m is the maximum adsorption at monolayer (mg g^{-1}), n is the adsorbent sets a limit to the maximum number of layers that can be adsorbed, x is the

equilibrium concentration of Au NPs (mg L^{-1}), and *c* is the BET constant expressive of the energy of interaction with surface.

Figure S1. ζ-potential determination in water solution. A, Native spores; B, Treated spores.

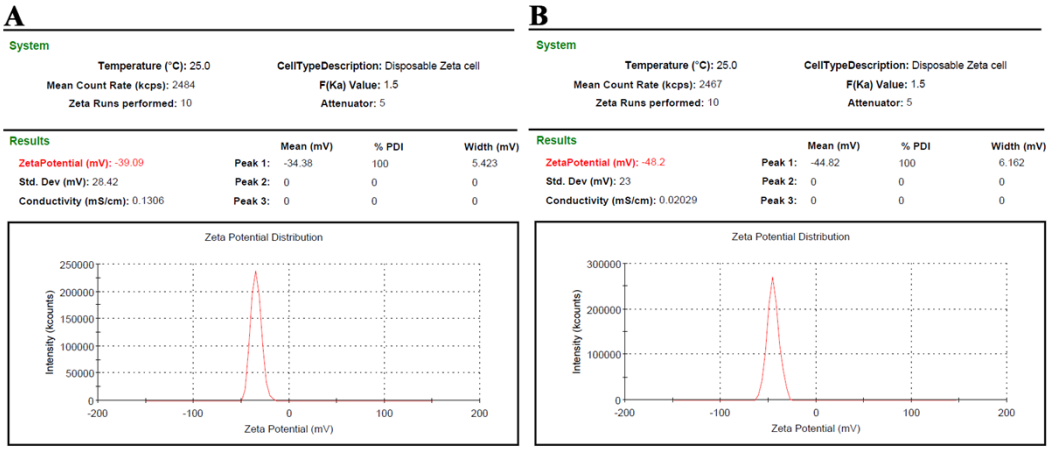

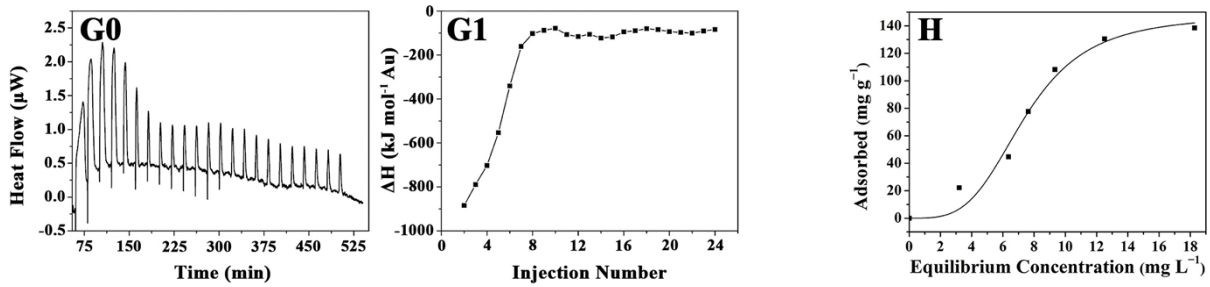

Figure S2. G) Power-time ITC thermogram for the addition of Au nanoparticles aqueous solution to treated spores suspension (G0) and the integrated heat data with an independent model fit (G1). H) Adsorption isotherms of Au nanoparticles onto treated spores.

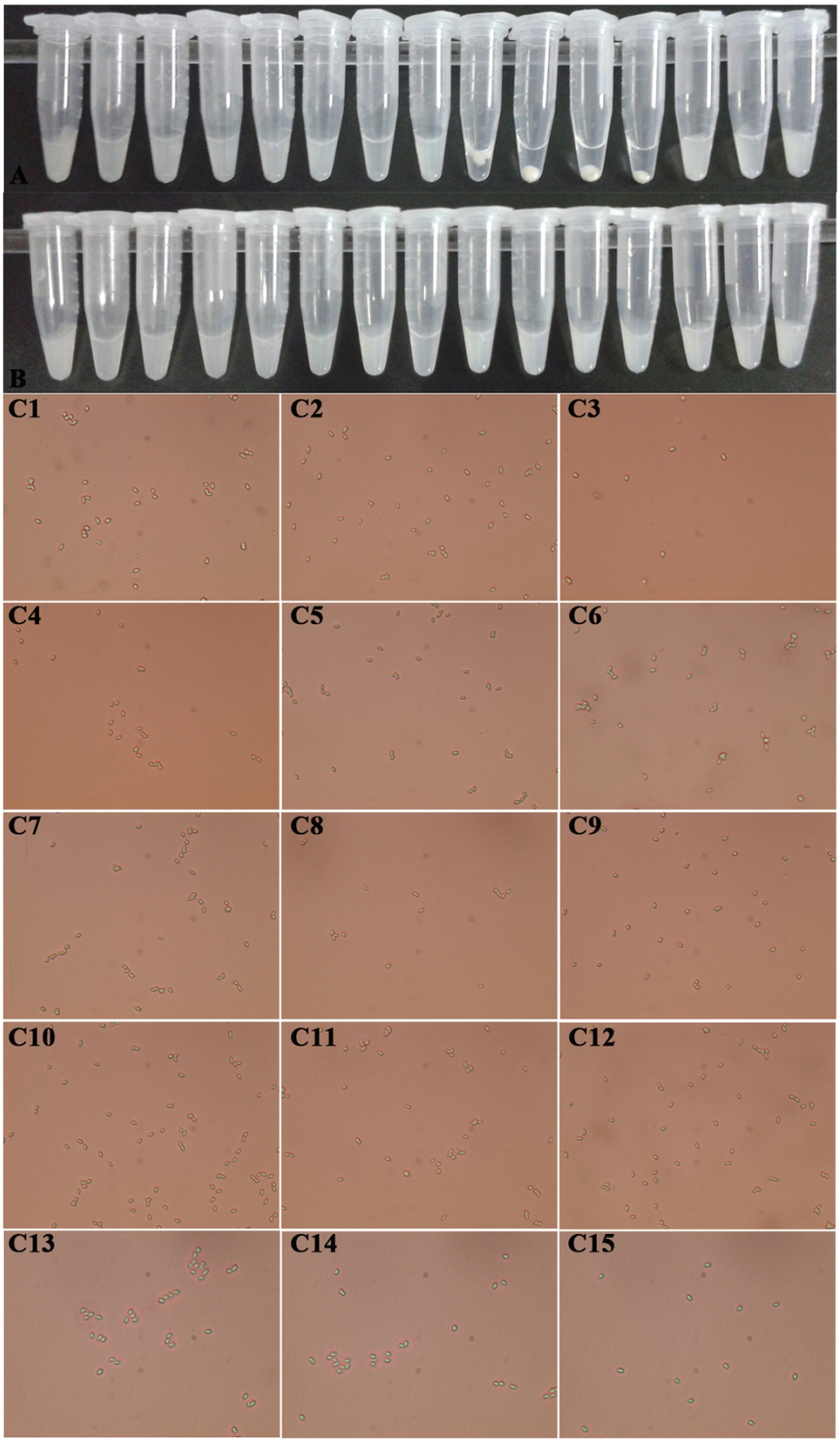

Figure S3. The dispersity and stability of TSs in different solvents, such as ethanol, methanol, acetone, formaldehyde, acetonitrile, formic acid, dimethylformamide, chloroform, toluene, hexane, cyclohexane, 0.5 mol L^{-1} and 0.1 mol L^{-1} HCl aqueous solution, and 0.1 mol L^{-1} NaOH aqueous solution.

Optimization of the immunoassay conditions

The influence of the immunoassay conditions was evaluated by measuring the F_0/F value (where, F_0 and F are the fluorescence intensities of standard positive and negative serum, respectively, measured at the same dilution ratio). The effect of Au microspheres concentration on the F_0/F value was determined by varying the concentration of Au microspheres from 1.24×10^9 CFU mL^{-1} to 7.41×10^9 CFU mL^{-1}. As shown in Figure S3A, F_0/F was enhanced as the concentration increased to 4.94×10^9 CFU mL^{-1}. At this concentration, F_0/F reached its maximum and began to decline thereafter. This result indicated that an excess of Au microspheres would decrease the detection sensitivity. The reason could be explained that when the number of Au microspheres greatly exceeded the number of ApxIVA protein, individual Au microspheres would capture much less ApxIVA protein and therefore could not be detected by the FCM, resulting in a decreased sensitivity. Consequently, the Au microspheres (4.94×10^9 CFU mL^{-1}) were added to subsequent experiments.

The influence of blocking buffer concentration and blocking time were also investigated. For BSA concentrations between 5 to 40 mg mL^{-1} inclusive, as shown in Figure S3B, the F_0/F value increased with BSA concentration up to 20 mg mL^{-1}. Further addition of BSA did not enhance the value. For blocking time from 0.5 h to 2.5 h, Figure S3C demonstrated that F_0/F value was the best at 1.5 h and decreased slightly since then. This could be interpreted that at a low BSA concentration and short time, the blocking of Au microspheres was not complete, resulting in the nonspecific binding and increasing the F value. However, more BSA concentration and blocking time brought about excessive BSA cover ApxIVA protein which attached to the surface of Au microspheres. As a result of this, the F_0 value was reduced. Therefore, 20 mg mL^{-1} was the optimal BSA concentration and 1.5 h was the appropriate blocking time in our experiments.

The optimal biotin-IgG concentration was determined by varying the antibody concentration from 0.25 to 2.5 μg mL^{-1}. Figure S3D illustrated that the F_0/F value increased gradually with the increase of biotin-IgG proportion and reached a plateau when 1.0 μg mL^{-1} antibody was used in this study. The reason may be that high concentrations antibody enhanced the nonspecific adsorption of biotin-IgG on Au microspheres. Therefore, F continually increased when the concentration of biotin-IgG higher than 0.1 μg mL^{-1}, and leading to the decrease of F_0/F. Accordingly, 0.1 μg mL^{-1} of biotin-IgG was then used in further experiments.

The fluorescence intensity was dependent only on the quantity of Cy™5 which was conjugated with streptavidin. To obtain the optimal streptavidin concentration, this quantity was varied from 0.05 to 2.0 μg mL^{-1}, and the results were shown in Figure S3E. The F_0/F value increased with increasing SA-Cy5 concentration within the range (0.05-0.5) μg mL^{-1}. Optimal F_0/F was achieved for SA-Cy5 concentration 0.5 μg mL^{-1}. Higher SA-Cy5 concentrations caused a decrease in F_0/F, probably due to the nonspecific adsorption of SA-Cy5 onto the surface of Au microspheres, which caused the F value to increase faster than F_0. Therefore, the SA-Cy5 concentration used in the experiments was 0.5 μg mL^{-1}.

A series of repeatability measurements of using 1:640-fold diluted standard positive serum gave reproducible results with a relative standard deviation (RSD) of 4.1% (n=11).

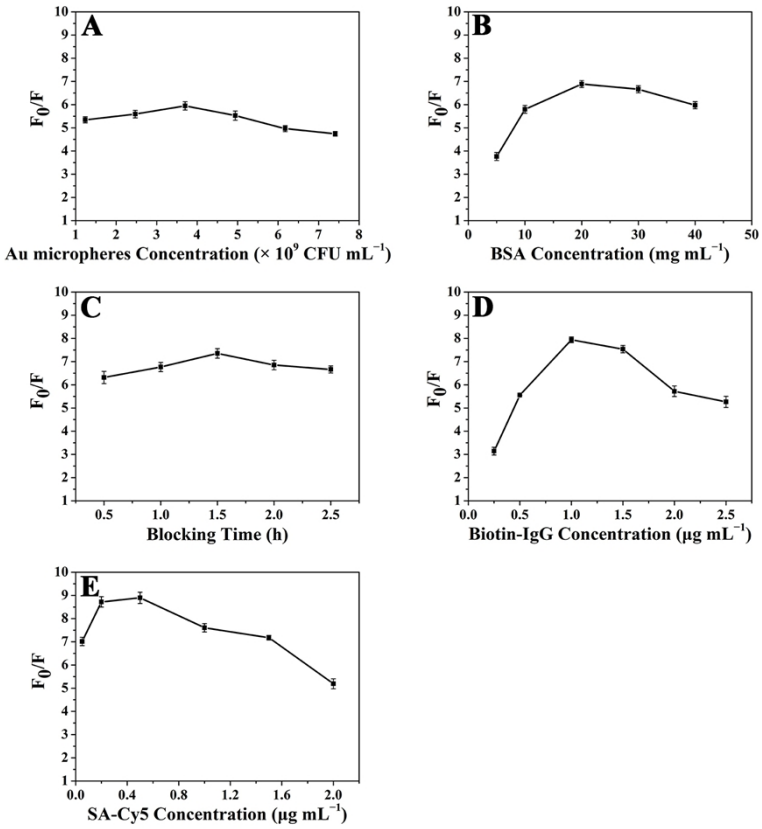

Figure S4. Effects of various conditions on the variance in fluorescence intensities ratio of F_0/F (where, F_0 and F are the fluorescence intensities of standard positive and negative serum, respectively, measured at the same dilution ratio). (A) Effect of Au microspheres concentration. Conditions: 10 mg mL^{-1} BSA; 1.0 h blocking time; 1:5120-fold diluted serum; 1.5 μg mL^{-1} biotin-IgG; 1.0 μg mL^{-1} SA-Cy5. (B) Effect of BSA concentration. Conditions: 3.705×10^9 CFU mL^{-1} spore; other conditions were the same as in Figure S3A. (C) Effect of blocking time. Conditions: 3.705×10^9 CFU mL^{-1} spore; 20 mg mL^{-1} BSA; other conditions were the same as in Figure S3A. (D) Effect of biotin-IgG concentration. Conditions: 3.705×10^9 CFU mL^{-1} spore; 20 mg mL^{-1} BSA; 1.5 h blocking time; other conditions were the same as in Figure S3A. (E) Effect of SA-Cy5 concentration. Conditions: 3.705×10^9 CFU mL^{-1} spore; 20 mg mL^{-1} BSA; 1.5 h blocking time; 1.0 μg mL^{-1} biotin-IgG; other conditions were the same as in Figure S3A. Error bars indicate the standard deviations from three independent measurements.

Table S1. Comparative results between Flow cytometry and ApxIVA-ELISA of 54 clinical serum samples

		Flow cytometry			Performance		
		Positive	Negative	Total	Efficiency (%)	Sensitivity (%)	Specificity (%)
ApxIVA-ELISA	Positive	25	2	27	88.9	92.6	85.2
	Negative	4	23	27			
	Total	29	25	54			

The efficiency, sensitivity and specificity values were calculated as follows: Efficiency = (TP + TN) × 100/Total = 88.9 (TP = 25, TN = 23, Total = 54); Sensitivity = TP × 100/(TP + FN) = 92.6 (TP = 25, FN = 2); Specificity = TN × 100/(TN + FP) = 85.2 (TN = 23, FP = 4) TP: True Positive; TN: True Negative; FP: False Positive; FN: False Negative.

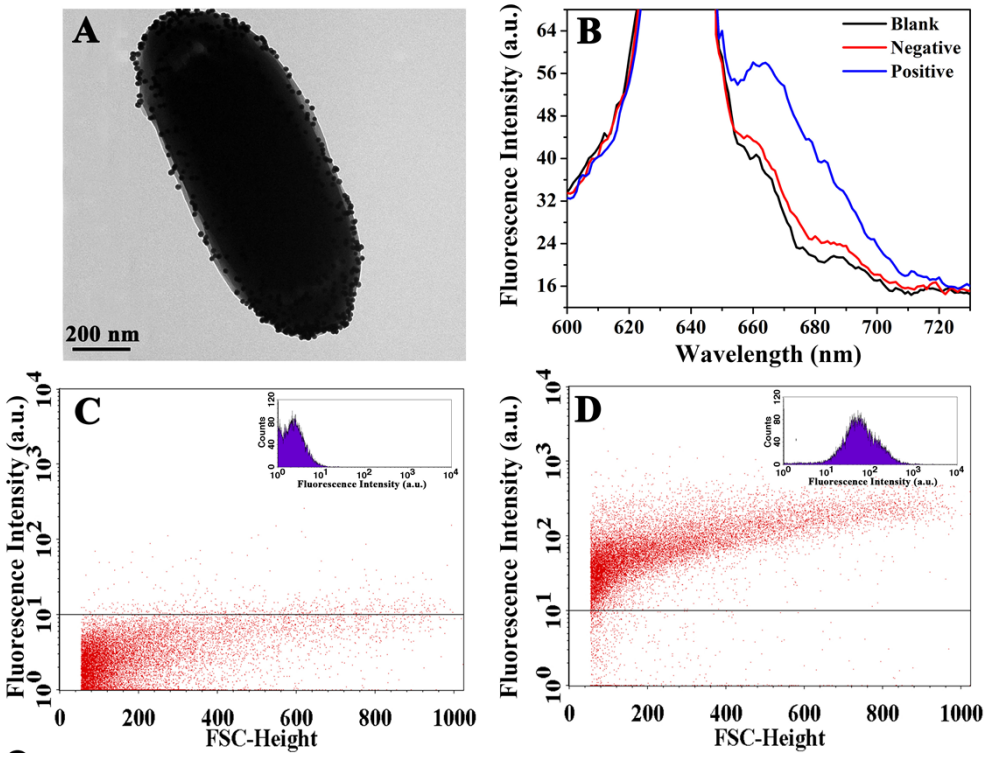

Figure S5. Application of Au microspheres for immunoassay. TEM images of Au microsphers (0.8 wt% Au). B) Fluorescence spectra of immunoassay for APP infection events. C) Dot and histogram (inset) of Au microspheres with negative serum. D) Dot and histogram (inset) of Au microspheres with positive serum. Conditions of B–D: Spore: 4.94×10^{9} CFU mL^{-1}; BSA: 10 mg mL^{-1}; Blocking time: 1.0 h; Negative serum: 1:320; Biotin-IgG: 1.5 μg mL^{-1}; SA-Cy5: 1.0 μg mL^{-1}.

Catalytic experiments

The amount of NPs present in the sample was determined using inductively coupled plasma-atomic emission spectrometry (ICP-AES). The light yellow aqueous 4-NP solution displayed a maximum absorption at 317 nm. After the addition of $NaBH_4$, the absorption maximum shifted to 400 nm due to the formation of 4-nitrophenolate ions. Visually, the bright-yellow solution gradually became colorless within 8 min.

The reaction rate constant k could be calculated from the rate equation:

$$\ln(C_t/C_0) = kt \quad (3)$$

Wherein, C_t and C_0 are 4-NP concentrations at time t and 0, respectively.

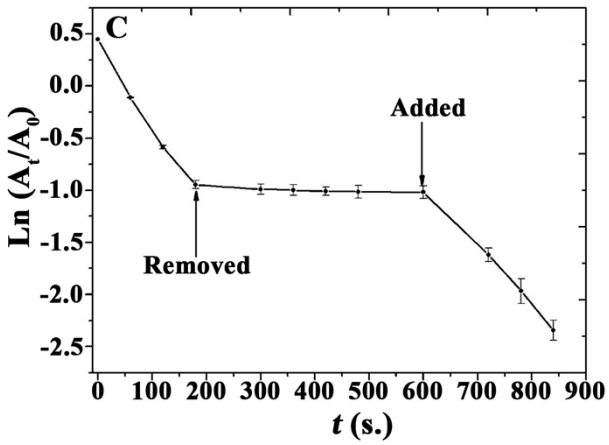

Figure S6. Plot of $\ln(A_t)$ as a function of time (t), in an experiment in which the catalyst were removed and re-added.